Development and Implementation of a Low-Cost Research Platform for Control Applications for Inverter-Based Generators

Jesus D. Vasquez Plaza, Juan F. Patarroyo-Montenegro, and Fabio Andrade
Dept. of Electrical and Computer Engineering
University of Puerto Rico at Mayagüez Campus
Mayagüez, Puerto Rico
E-Mail: jesus.vasquez@upr.edu, juan.patarroyo@upr.edu, and
fabio.andrade@upr.edu
URL: https://inec.uprm.edu/sec/

Keywords

«Research platform», «Microcontroller», «LC-Filter», «Resonant Controller»

Abstract

This document presents the develop and implementation of a low-cost research platform based on a microcontroller. The platform was validated through implementation of a resonant controller in $\alpha\beta$ -frame for Inverter-Based Generators. Also, this work proposes a comparative analysis between a dSPACE 1006 and the embedded systems for control applications in inverter-based generators (IBGs). For the development of the research platform, a microcontroller from the Texas Instruments TMS320F28379D C2000 line was used. Our analysis revealed that control behavior for IBG applications through a low-cost platform based on a microcontroller is similar to that of a dSPACE.

Introduction

In recent times, the use of renewable energy sources is increasing dramatically worldwide. This has led to the questioning about sustainability of traditional electric power systems since they are mainly based on the generation of fossil fuels (oil, coal, natural gas). The environmental needs are increasingly demanding a change of the energetic paradigm due to the negative impact that fossil fuels cause. Thanks to the inclusion of renewable energy, the concept of microgrid is becoming popular. Thus, the use of Inverter-based Generators (IBG) is more common nowadays.

A microgrid can work in two operating modes: grid connected or in isolated mode. To achieve optimal operation, the microgrids need advanced control strategies to guarantee the voltage and frequency levels in any of the operating modes. A flexible platform that can operate in both operating modes without any significant changes in hardware is ideal for research and education issues

Currently, the control of microgrids is a source of continuous research, specifically in the control of IBG. That is why companies like OPAL RT, National Instruments, dSPACE Typhoon, RTSD, RT Box Plexim, etc., are increasing their offer with respect to Hardware-in-the-Loop (HIL) systems. These companies provide multiple modules to simulate real-time energy systems. These technologies allow research centers to improve their infrastructure and, in this way, they emulate and solve problems regarding to renewable energies. In [1], [2], [3] and [4] some works relating to the development, implementation and analysis of controllers of power electronic systems in which they use HIL technologies are presented.

Although these tools are very powerful, they are expensive as well. Therefore, they are difficult to access by low-income universities that belong to developing countries. This paper aims to present a low-cost microcontroller-based platform that allows for the implementation of advanced control strategies for IBG. Also, this project presents the development of a comparative analysis in terms of performance with respect to one of the HIL tools mentioned above, specifically a dSPACE 1006.

Microcontroller-Based Research Platform for IGB Control Applications

For the development of the research platform for IBGs, we developed a control box (CBOX) based on a microcontroller. This control box is composed of a Texas Instruments (TI) C2000 TMS320F28379D microcontroller (uC), custom made analog signal conditioning board and electrical signal to light pulses conversion board (optical fiber). Aditionally, a IBG Danfoss VLT-302 inverter and a SensorBox were used, the last two supplied by the Sustainable Enegy Center (SEC) of the University of Puerto Rico de Mayaguez (UPRM). The CBOX contains all the necessary ports to connect to the SensorBox and the IBG to perform the respective control. A set of experiments was developed to program and interact in real time with the uC through the blocks and tools provided by the Simulink-Matlab visual programming environment. These experiments validated the different peripherals of the uC (ADCs, Digital Input/Output, etc.) and implemented the desired control strategies for the control of IBGs. In addition, Matlab offers a work environment called GUIDE [5] allowed to design a custom user interface, a dragand-drop environment to observe the values of the controller variables in real-time and to change the parameters of the controller on the fly, if necessary. A general description of the developed platform is shown in Fig 1.

The CBOX uses a C2000 TMS320F28379D microcontroller. It operates at 200MHz and is equipped with 24 analog-to-digital (ADC) conversion channels with a resolution of 12 bits, 16 independent 32-bit PWM channels, floating point unit (FPU), JTAG emulation tool and other features that make this microcontroller ideal for high capacity digital control purposes in IBG applications.

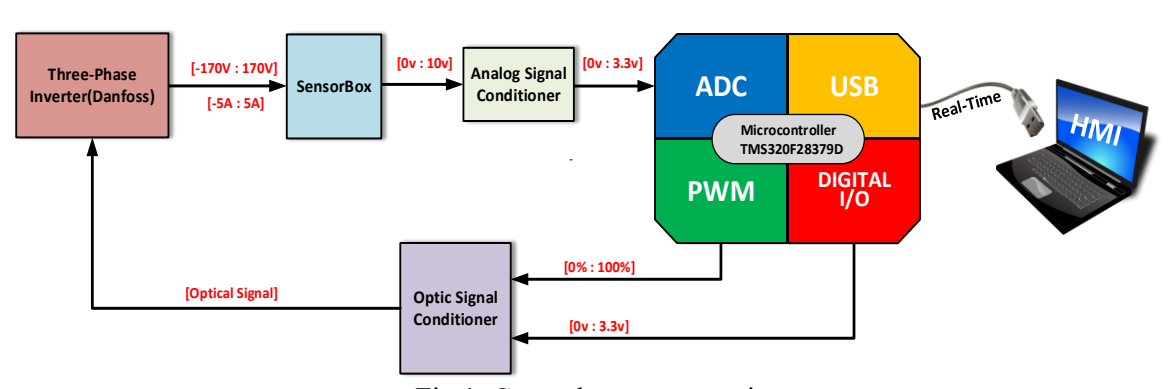


Fig 1. General system overview

System Assembly

The three boards contain in the CBOX are describe as follow: first, analog signal conditioning board is required to convert the voltage signal levels from the SensorBox into a range that the microcontroller can read (0-3.3V). The CBOX is packaged in an enclosure which was designed in SolidWorks and made by a 3D printer. It contains a port to connect it to the conventional grid (120Vac), a USB port to communicate and program the uC in Real-Time, 14 ports for analogue signal input from the SensorBox, 5 output ports and 1 input for optical signals to control the IBG. The CBOX was designed with 14 channels that allow analog signals to be read simultaneously, from the SensorBox. The SensorBox was originally designed to convert the measured signals into a range of voltage levels from -10V to + 10V. For this reason, a signal conditioner circuit is used to convert these voltage levels to a range of 0V to 3.3V, which is the operating range of the ADC unit of the uC. To achieve this objective, it was necessary to attenuate and add an offset value to the signals coming from the SensorBox in order to convert them into positive unipolar signals to read it properly with the uC. The OP482 amplifier from Analog Devices was used for this task because it has a high response speed ($9V/\mu s$), wide bandwidth (4 MHz), low noise and other features that make it ideal for this application. this amplifier has 4 independent channels with high response speeds.

To generate an attenuation of 0.15, resistors of RD=150 Ω and RC=1k Ω were used Fig 2 shows the proposed design of the analog signal conditioning circuit. The output voltage is given by (1).

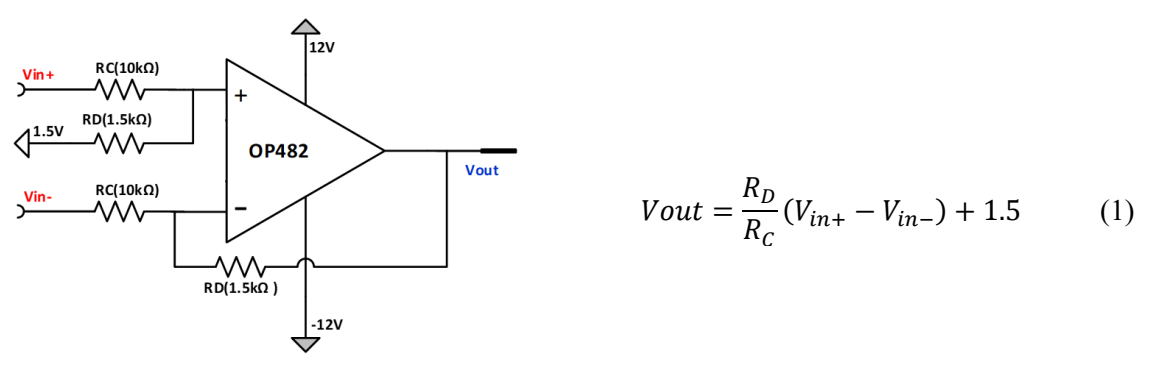


Fig 2. Analog signal conditioning circuit

Second, Optical Signal Conditioning Board is required to convert the PWM (electrical signals) into light signals, which will be responsible for carrying the control signals to the IBG, this board receives electrical signals and transforms them into light signals, has 6 optical signal ports, 5 outputs and 1 input. The 5 optical output signals are distributed as follows: 3 signals are from PWM responsible for applying the control signals to the IBG; a Reset signal to reset the IBG in case it is blocked a non-lethal fault; and an Enable signal for activating or deactivating the IBG. On the other hand, the input signal called TRIP informs the IBG had a fault and is blocked. This board is interconnected with the Analog Signal Conditioning Board through a ribbon cable.

Finally, BNC Signals Board is required to connect to 14 BNC channels of the SensorBox output ports. This board is connected to the Analog Signal Conditioning Board using a ribbon cable. In short, this card serves as an interface between the SensorBox and the Analog Signal Conditioning.

Fig 3 shows the final assembly of the CBOX. The CBOX is organized so that its main modules can be visually identified and used with little risk of damage.



Fig 3. Final box assembly of the CBOX. Left: internal view. Right: external view

Graphic Interface

Grafic Interfaces allow easy control of software applications, which eliminates the need to learn a programming language and write commands in order to run an application. With the help of Matlab GUIDE, an interface was created that allows you to program the uC with files previously created from Simulink and at the same time observe and change the parameters of the controllers that were implemented. For each type of controller implemented in this platform, different interface were developed.

Fig 4 shows the interface developed for the $\alpha\beta$ controller, which will be discussed later. As you can be seen, the interface consists of 4 sections that will be described below.

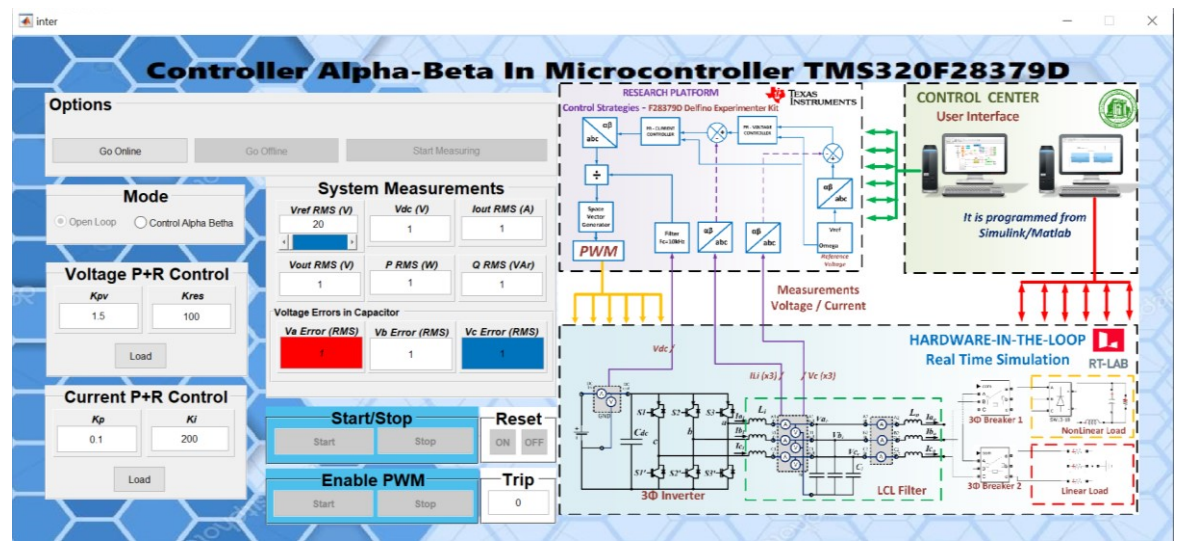


Fig 4.User interface for the microcontroller-based platform for IBG control applications

The *Options* section contains three buttons.

- The "Go Online" button allows you to program the uC with the control strategy and keep the system running in real-time.
- The "Go Offline" button allows you to reset the uC and finish the data transmission in Real-Time.
- The "Start Measuring" button allows you to display some variables of interest on the screen in real-time, such as the dc bus voltage (Vdc), RMS value of the IBG output current (Iout), RMS value of the voltage of IBG output (Vout), Ppower that is delivering the IBG (P RMS) and voltage errors with respect to the reference (Va, Vb, Vc RMS Error).

The *Mode* section allows you to switch between the type of control strategy or the open loop system without a controller.

The *System Measurements* section allows visualizing on display the variables of interest in real-time at the moment the "*Start Measurement*" button is pressed. It also contains a slider bar that allows you to vary the reference voltage for the IBG between 20 and 120 volts RMS as desired, it is also accompanied by a display (Vref) where you can enter numerically and observe the value of the voltage reference. Finally, the section of *Voltage and Current P+R* Control allows to visualize and change the values of the voltage parameters and current controllers (*Kpv, Kres, Kp, Ki*) as desired, the selection of these values will be farther discussed.

Platform Validation

To validate the correct functioning of the platform, a three-phase inverter with an LCL filter was used. The platform was validated by controlling the voltage in the capacitors (Ci) and the current control in the input inductance (Li).

In order to control the inverter, it is necessary to measure the signals of interest, which is achieved with the SensorBox described above. Once the signals of interest are measured, they are sent to the uC, which is responsible for carrying out the respective control and generating the PWM signals that will switch the inverter's power transistors and obtain the desired output voltage.

In Fig 5, a general scheme of the inverter with the LCL filter and a load is observed. In addition, all the voltage and current measurements necessary to control the inverter are observed. On the other hand, the PWM block represents the optical signals from the optical signal conditioning board.

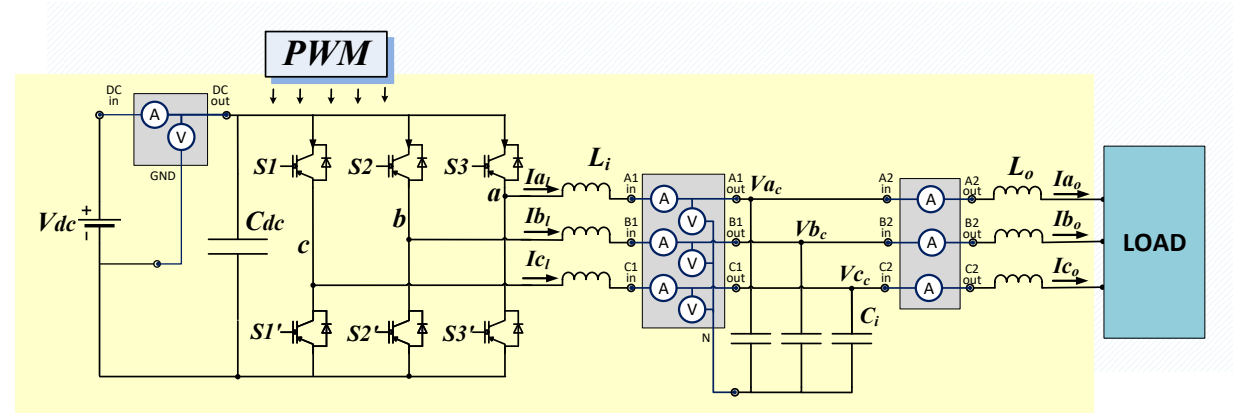


Fig 5. General scheme of the three-phase inverter with LCL filter

The model of the inverter is represented in equations of state. For simplicity of the model and control of the three phase inverters, the $\alpha\beta$ transform is used in the reference frame aligned to the voltage in the capacitor of the LC filter. The LC filter model is given by the following equations:

$$\begin{bmatrix} \dot{V}_c \\ i_t \end{bmatrix} = \begin{bmatrix} 0 & \frac{1}{C} \\ -\frac{1}{L_i} & -\frac{Ri}{L_i} \end{bmatrix} * \begin{bmatrix} V_c \\ i_t \end{bmatrix} + \begin{bmatrix} 0 \\ \frac{1}{L_i} \end{bmatrix} * V_{ref}$$
 (2)

To validate the platform the resonant control in $\alpha\beta$ -frame was selected, work related to the implementation of these controllers is described in [6]–[9]. shows the general scheme of the system with PR control ($\alpha\beta$), in which there is an internal loop that controls the circulating current by Li and an external voltage loop that controls the voltage in the capacitor Vc.

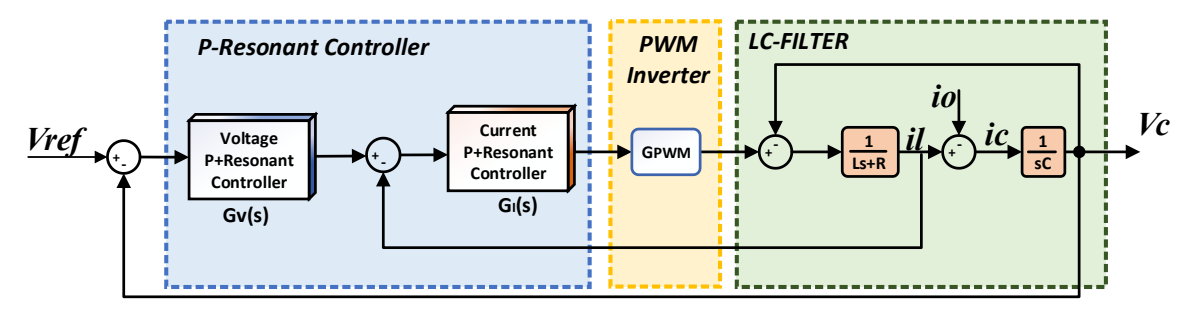


Fig 6. General schematic of the IBG with PR ($\alpha\beta$) current and voltage controller

where the GPWM transfer function corresponds to the delay due to the calculation device (Ts) and the PWM (0.5Ts), with Ts being the sample period. The GPWM transfer function is given by:

$$G_{PWM}(s) = \frac{1}{1 + 1.5T_S s} \tag{3}$$

The transfer functions GV (s) and GI (s) correspond to the PR controllers of voltage and current, respectively. The main characteristic of these controllers is that it has an infinite magnitude gain in its resonant frequency ω , and it presents an abrupt 180 phase change in the frequency ω . The equations G_V (s) and G_I (s) are given by (4) and (5), where K_{pv} - K_{pi} and K_{iv} - K_{ii} are the proportional and resonant constants for current and voltage controllers, respectively. $\omega 0$ is the desired resonant frequency, in this almost 377rad/s [10][11].

$$G_{v}(s) = K_{pv} + \frac{K_{iv}s}{s^{2} + \omega_{0}^{2}} \qquad G_{i}(s) = K_{pi} + \frac{K_{ii}s}{s^{2} + \omega_{0}^{2}}$$
(4)

For the controller mentioned above, the design and calculation of their parameters was carried out by means of the frequency response using the bode diagrams as in [10]. **Table 1** shows the values of the system parameters to be controlled.

| Parameters | Symbol | Nominal Value |
|----------------------|--------------|---------------|
| Switching frequency | fs | 10kHz |
| Sampling Time | Ts | 100μs |
| Filter inductance | Li - Lo | 1.8mH |
| Filter capacitance | С | $8.8\mu F$ |
| LC Filter resistance | R_i | 2Ω |
| System frequency | ω_{o} | 2*pi*60 rad/s |

Table 1. System Parameters

The constants of the PR controllers obtained for the current and voltage controller were $K_{pi}=0.1$ - $K_{ii}=200$ and $K_{pv}=1.5$ - $K_{iv}=100$, respectively.

Experimental Results

Prior to experimental implementation, to carry out the comparative analysis of the platform developed in this investigation with respect to a HIL technology, it was necessary to validate the system with the simulation strategies described. For this reason, the MATLAB-Simulink tool was used, which allows executing complex system simulations with precision.

Subsequently, to evaluate the performance of the proposed research platform, one of the inverters of the SEC-UPRM microgrid test bench was used [12]. The experimental setup is represented in Fig 7 consisted of a 2.2kW Danfoss inverter, an LCL filter, a CBOX or dSPACE, and a SensorBox. The switching frequency of the inverter was adjusted to 10 kHz by symmetric spatial vector modulation. Finally, the voltage in the capacitors (Vc) was acquired using a Lecroy Wavesurfer 64Xs oscilloscope, which allows the measured signals to be converted into data that can be processed in Matlab. For validation, our platform was compared to the behavior of the dSPACE 1006. In the two systems, the same controller was implemented with the same parameters, the same inverter was controlled with the same LCL filter.

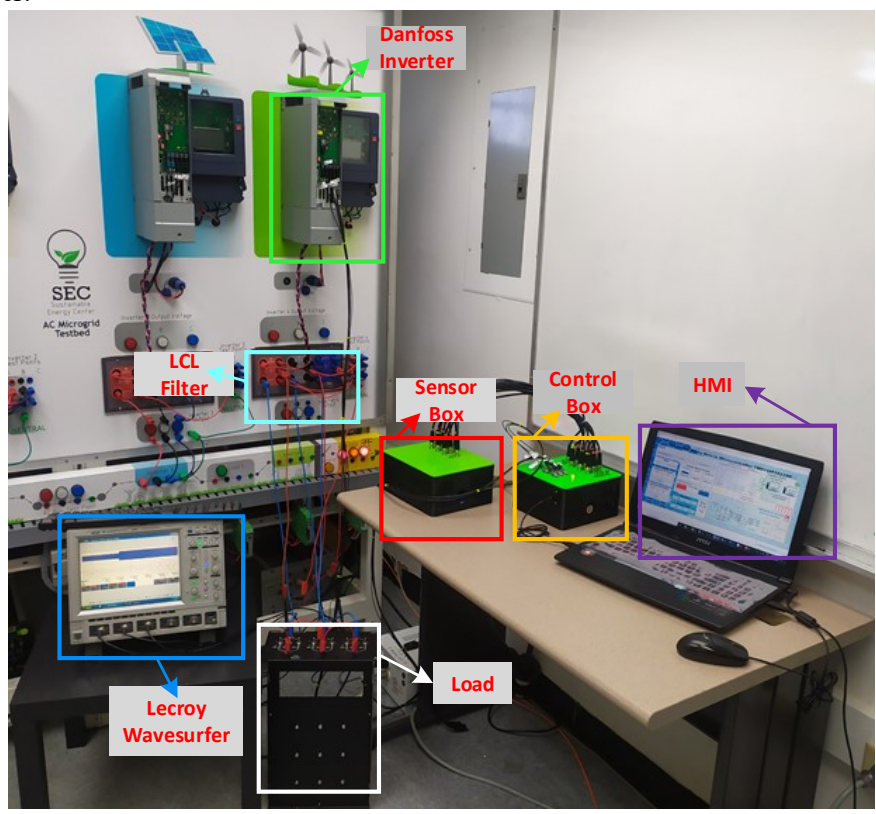


Fig 7. Experimental Low-Cost Research Platform

The experimental results of the PR ($\alpha\beta$ -frame) control implemented was validated for both the CBOX and a the dSPACE. Fig 8 shows the voltage behavior in the capacitor for the controllerless system with our platform and the dSPACE.

The voltage reference was initially set at 60V RMS. After 1 second, a 60V step was used to reach the voltage of the conventional grid (120V RMS). It was observed that the transient in the simulated model had more harmonic components as in the open loop model because the simulation did not consider all damping factors. It is observed that the behavior of Vc controlled by our platform and by dSPACE had a similar dynamic. The simulated system had a settling time of 15ms, and a maximum exceeding of 7V with respect to the reference (less than 5%). The system controlled by our platform and the dSPACE behaved in a similar way and had a maximum overshoot in one of its 15V phases (less than 10%) and also presented a maximum error of 5V in steady state, that is, an error of less than 3%. The exact similarity values between our platform and the dSPACE when implementing the $\alpha\beta$ controller will be presented in the next section.

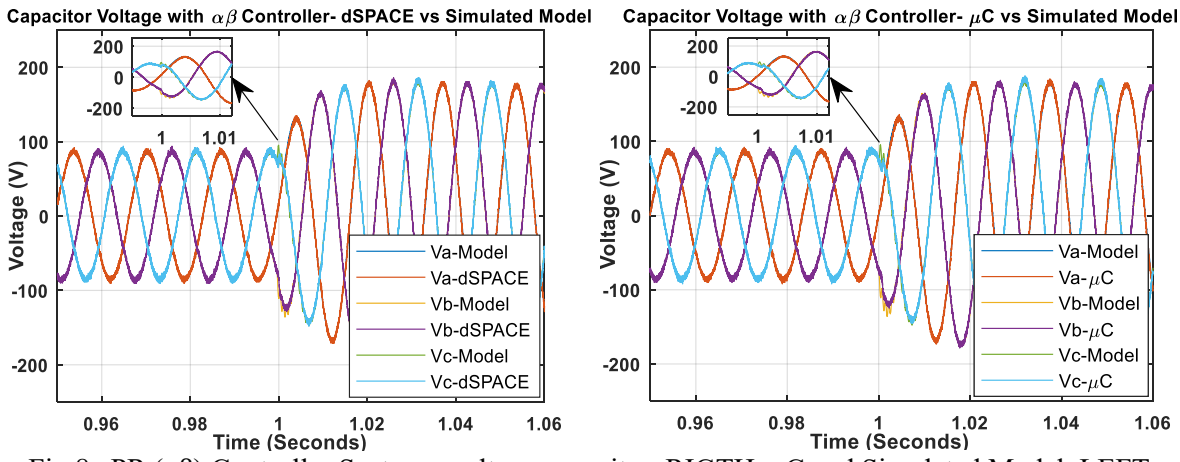


Fig 8. PR (αβ) Controller System - voltage capacitor. RIGTH: uC and Simulated Model. LEFT: dSPACE and Simulated Model

Comparative Analysis

For the PR ($\alpha\beta$ -frame) controller implemented in our platform and in a dSPACE 1006 the voltage signals in the capacitor (Vc) is compared, which is superimposed and compared with respect to the Vc of the simulated model in a time interval determined.

For each platform with respect to the simulated model, the root mean normalized square error (NRMSE) is defined by [13].

$$NRMSE = 100 \times \left(1 - \frac{\left\|Vc_{ref} - Vc_{Pl}\right\|}{\left\|Vc_{ref} - mean(Vc_{ref})\right\|^{2}}\right).$$
 (5)

where $\|.\|$ Indicates Euclidian norm of a vector. The vectors Vc_{Pl} and Vc_{ref} represent the Vc for each platform and the Vc of the simulated model, respectively. The NRMSE is suitable for this validation because it considers the complete measurement during a specific time interval. This means that it is suitable for comparing responses with a high frequency component, such as signals from an IBG that operates at high frequencies. Fig 9 shows the NRMSE for the system with PR controller ($\alpha\beta$ -frame) All adjustment values are above 96% in each of the phases of Vc with respect to the simulated model. In addition, the system controlled by the uC has an error rate of less than 1% with respect to the dSPACE when compared to the simulated model. These results demonstrate that our platform has the ability to keep the IBG stable and controlled through the implementation of the $\alpha\beta$ controller, obtaining results similar to those of dSPACE.

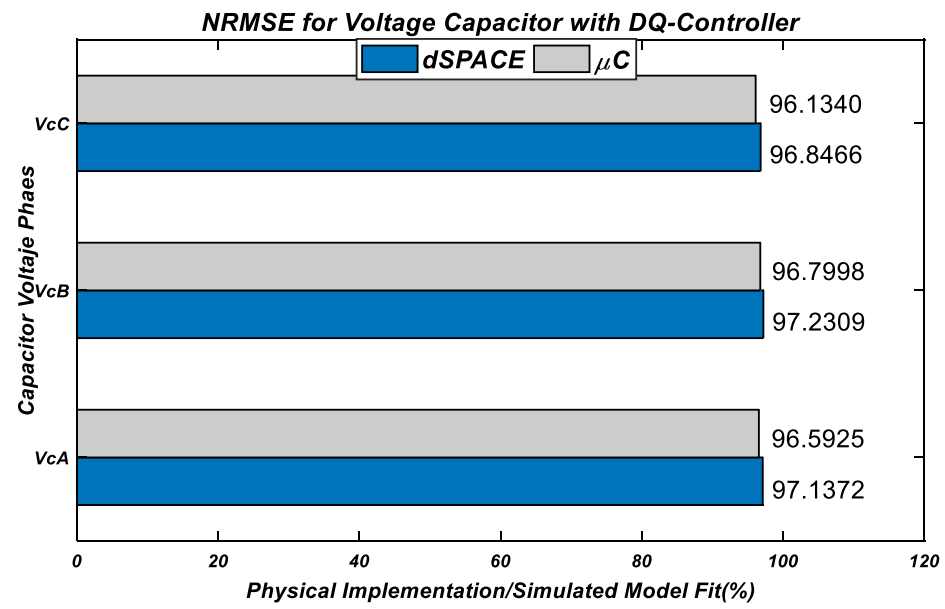


Fig 9. NRSME for capacitor voltage between simulated model and uC - dSPACE with PR ($\alpha\beta$ -frame) controller

Through the results obtained when applying the NPSME to the Vc Voltage obtained with our uC-based platform, as well as when implementing PR ($\alpha\beta$ -frame) controller in the dSPACE with a real IBG, we observed that the errors regarding the dSPACE in all the cases were less than 1% with respect to the simulated model. These results demonstrate that our platform has the capabilities to implement control strategies for IBG applications, obtaining results similar to that of the dSPACE.

On the other hand, when directly comparing our platform and the dSPACE, NRSME values of 97.25%, 96.79%, and 96.93 are obtained for the three phases of the voltage in the capacitor *VcA*, *VcB*, and *VcC*, respectively.

According to our criteria, it is considered that a value greater than 85% similarity between our platform and the dSPACE is sufficient to determine that the platform meets the requirements to implement control strategies for IBG applications. The results obtained demonstrate that our platform has the capacity to implement controllers for IBG applications, since through the implementation of the ab and dq controller there is a stable and contracted system with a percentage of similarity greater than the threshold (85%) established with respect to a dSPACE 1006.

Conclusion

By implementing a PR ($\alpha\beta$ -frame) controller for IBG applications through a low-cost uC-based platform, a similar behavior is obtained as when implementing the controllers with high-performance technologies. The comparative analysis carried out demonstrates that the results obtained with our platform based on a uC and the dSPACE 1006 are similar. The platform proposed in this work allows for the research and implementation of advanced control strategies for IBG to be accessible to universities with low budgets that are in the process of development.

References

- [1] M. Mobarrez, N. Ghanbari, and S. Bhattacharya, "Control Hardware-in-the-Loop Demonstration of a Building-Scale DC Microgrid Utilizing Distributed Control Algorithm," IEEE Power Energy Soc. Gen. Meet., vol. 2018-Augus, pp. 1–5, 2018.
- [2] S. Acharya, M. S. El Moursi, and A. Al-Hinai, "Coordinated Frequency Control Strategy for an Islanded Microgrid With Demand Side Management Capability," IEEE Trans. Energy Convers., vol. 33, no. 2, pp. 639–651, 2018.
- [3] A. Mortezaei, M. G. Simoes, A. S. Bubshait, T. D. C. Busarello, F. P. Marafao, and A. Al-Durra, "Multifunctional Control Strategy for Asymmetrical Cascaded H-Bridge Inverter in Microgrid Applications," IEEE Trans. Ind. Appl., vol. 53, no. 2, pp. 1538–1551, 2017.
- [4] A. S. Bubshait, A. Mortezaei, M. G. Simoes, and T. D. C. Busarello, "Power Quality Enhancement for a

- Grid Connected Wind Turbine Energy System," IEEE Trans. Ind. Appl., vol. 53, no. 3, pp. 2495–2505, 2017.
- [5] Matlab, "Create a Simple App Using GUIDE MATLAB & Simulink." [Online]. Available: https://www.mathworks.com/help/matlab/creating_guis/about-the-simple-guide-gui-example.html.
- [6] A. G. Yepes, F. D. Freijedo, J. Doval-Gandoy, Ó. López, J. Malvar, and P. Fernandez-Comesaña, "Effects of discretization methods on the performance of resonant controllers," IEEE Trans. Power Electron., vol. 25, no. 7, pp. 1692–1712, 2010.
- [7] F. D. Freijedo et al., "Grid-synchronization methods for power converters," IECON Proc. (Industrial Electron. Conf., no. December, pp. 522–529, 2009.
- [8] L. Antonio De Souza Ribeiro, F. D. Freijedo, F. De Bosio, M. Soares Lima, J. M. Guerrero, and M. Pastorelli, "Full Discrete Modeling, Controller Design, and Sensitivity Analysis for High-Performance Grid-Forming Converters in Islanded Microgrids," IEEE Trans. Ind. Appl., vol. 54, no. 6, pp. 6267–6278, 2018.
- [9] M. Bobrowska-Rafał, "Grid Synchronization and Control of Three-Level Three-Phase Grid-Connected Converters based on Symmetrical Components Extraction during Voltage Dips," PhD Thesis, p. 141, 2013.
- [10] J. C. Vasquez, J. M. Guerrero, M. Savaghebi, J. Eloy-Garcia, and R. Teodorescu, "Modeling, analysis, and design of stationary-reference-frame droop-controlled parallel three-phase voltage source inverters," IEEE Trans. Ind. Electron., vol. 60, no. 4, pp. 1271–1280, 2013.
- [11] R. Teodorescu, F. Blaabjerg, M. Liserre, and P. C. Loh, "Proportional-resonant controllers and filters for grid-connected voltage-source converters," vol. 150, no. 20030259, 2003.
- [12] J. F. Patarroyo-Montenegro, J. E. Salazar-Duque, S. I. Alzate-Drada, J. D. Vasquez-Plaza, and F. Andrade, "An AC Microgrid Testbed for Power Electronics Courses in the University of Puerto Rico at Mayagüez," 2018 IEEE ANDESCON, ANDESCON 2018 - Conf. Proc., pp. 1–6, 2018.
- [13] A. G. Barnston, "Correspondence among the correlation, RMSE, and Meidke Foresast verification measures; Refinement of the Neidke Score," Weather and Forecasting, vol. 7, no. 4. pp. 699–709, 1992.